5th International Conference
"Computational Mechanics and Virtual Engineering"
COMEC 2013
24- 25 October 2013, Braşov, Romania

ON THE EFFECTIVE MODULI OF SONIC COMPOSITES

Ligia Munteanu[1], Veturia Chiroiu[1], Ştefania Donescu[2], Ruxandra Ilie[2], Valerica Moşneguţu[1]
[1]Institute of Solid Mechanics, Ctin Mille 15, Bucharest 010141,
ligia_munteanu@hotmail.com, valeriam732000@yahoo.com
[2]Technical University of Civil Engineering, Bd. Lacul Tei nr.122-124, Bucharest 020396
stefania.donescu@yahoo.com, rux_i@yahoo.com

To the memory of Prof. Petre P. Teodorescu (1929-2013).
The Professor's name would forever be engraved in our hearts.

Abstract: *The auxetic behavior is interpreted in the light of Cosserat elasticity which admits degrees of freedom not present in classical elasticity, i.e. the rotation of points in the material, and a couple per unit area or the couple stress. The Young' modulus evaluation for a sonic composite designed in order to provide suppression of unwanted noise for jet engines, with emphases on the nacelle of turbofan engines for commercial aircraft, is presented in this paper.*
Key-Words: *Auxetic material, Cosserat elasticity, Young's modulus, sonic composite.*

1. INTRODUCTION

The sonic composites we discuss in this paper consist of an array of acoustic scatterers having the shape of spherical shells and made of the auxetic material (negative Poisson coefficient), embedded into the epoxy matrix. Let us begin with the auxetic materials, that have a negative Poisson ratio. The term *auxetic* is coming from the Greek word *auxetos*, meaning *that which may be increase*. Instead of getting thinner like an elongated elastic band, the auxetic material grows fatter, expanding laterally when stretched. All the major classes of materials (polymers, composites, metals, ceramics honeycomb structures, reticulated metal foams, re-entrant structures, the skin covering a cow's teats, certain rocks and minerals, living bone tissue) can exist in the auxetic form [1-6].
The idea is to transform a non-auxetic material into auxetic forms as foams or cellular materials, or to employ new techniques for architecture new auxetic materials.
The simulation of a sonic composite based on the auxetic materials was studied in [7] and [8]. We briefly describe in the following the principal results reported in [7] and [8] because the present paper is devoted to evaluate the Young'modulus for the sonic composite described in these papers.
These sonic composites are characterized by the existence of a large sound attenuation band which is done by the superposition of multiple reflected waves within the array according to the Bragg's theory. The band-gaps which characterises a sonic composite correspond to the Bragg reflections that occur at different frequencies inverse proportional to the central distance between two scaterers [7-9]. If the band-gaps are not wide enough, their frequency ranges do not overlap. These band-gaps can overlap due to reflections on the surface of the scatterers, as well as due to wave propagation inside them. Then, any wave is reflected completely from this periodic array in the frequency range where all the band-gaps for the different periodical directions overlap.
This is the fundamental mechanism for the formation of a full band-gap which is required for sonic composites. The complete reflection on the boundaries of scatterers is due to the full band-gap property itself, independent of the incident angle. This makes sharp bends of the wave-guide in the sonic composite. The evanescent waves distribute across the boundary of the waveguide into the surrounding composite by several times the lattice constant.
The geometry of the scatterers and the material of which they are made, are not assumed a priori. A new technique for choosing the geometry and the material for the acoustic scatterers, is proposed. This technique is performed in two stages. In the first stage, the acoustic scatterer is the traditional one, i.e. a sphere filled with conventional foam with positive Poisson ratio. In the second stage, a new geometry and a new material are looking for the scatterer so that the efficiency of the sonic line to be high. The achieving of this stage is made as simple and inexpensive as the first one.
The secret is the property of the equations that describe the behavior of the conventional sonic line. These equations can be reduced to Helmholtz equations which are invariant under geometric transformations. In other words, by

choosing an appropriate geometric transformation, the conventional foam-filled sphere can be changed into a new scatterer with different geometry filled with a new material obtained from the initial one by spatial compression.
We must specify that the auxetic foam manufacturing relies on the compression of the conventional one. The conventional foam has pores with an average diameter of around 900, with an isotropic distribution of the major axis of the cell in different directions. The manufacturing of auxetic materials is based on the cell size reduction through radial compression molds.
Therefore, by a careful handling of the geometric transformation we can lead to a simple, cheap and efficient simulation of the manufacturing process of the material required for a high reduction / removal of the noise in the sonic line. The proposed technique is based on the Cosserat theory combined with cnoidal method and a genetic algorithm, respectively.
The standard continuum models cannot describe the phenomenon of band- gaps (the regions in the frequency-wavenumber space where the energy does not propagate) for heterogeneous materials that appear to be homogeneous at the meso-scale. The Cosserat or micropolar theory is an alternative continuum model that incorporate a length scale.
The conventional foams are materials with microstructure which exhibit chiral effects. These effects cannot be expressed within the classical elasticity since the modulus tensor, which is of the fourth rank, is unchanged under inversion

$$C_{ijkl} = x_{m,i}x_{n,j}x_{o,k}x_{p,l}C_{mnop} = (-1)\delta_{im}(-1)\delta_{jn}(-1)\delta_{ok}(-1)\delta_{pl}C_{mnop} = (-1)^4 C_{ijkl} = C_{ijkl}\,. \tag{1}$$

This provides a motivation towards developing enriched continuum models endowed with intrinsic length scales that synthesize the key features of the sub-scale material architecture. This is the reason we have chose to describe the chiral properties to Cosserat elasticity [10], [11].

2. THEORY

Let us consider a liner consisted of a porous or perforated facing sheet forming the interior duct wall, bonded on a composite layer and is terminated with a rigid back wall (Figure 1) [8]. The composite layer is a thin plate consisting of an array of acoustic scatterers embedded in an epoxy matrix. The acoustic scatterers are spheres made from conventional foam and the matrix is made from an epoxy resin (Figure 2).
The plate consists of 144 local spherical resonators of diameter a. The length of the plate is L, its width is d, while the diameter of the sphere is a and its thickness is $e > a$. The purpose of this sonic liner is to suppress the noise generated by the fan before it radiates out of the fan inlet and the fan exhaust ducts and in some instances, to reduce the combustion and turbine noise in the exhaust duct of the core engine.

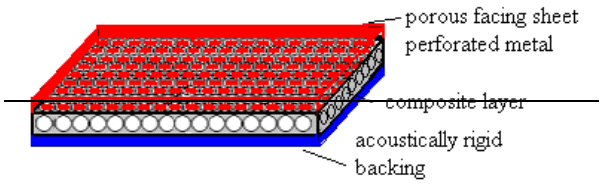

Figure 1: The plate with spherical resonators [8]

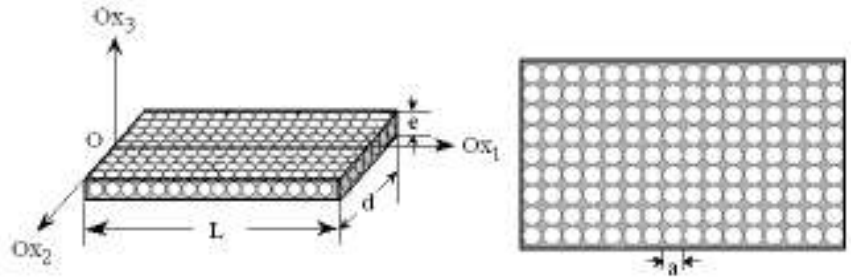

Figure 2: Sketch of the composite layer with spherical scatterers [8]

Consider a chiral Cosserat medium, in a Cartesian coordinates system $x \equiv (x, y, z)$. The equations of motion for the case without body forces and body couples are [12]-[15]

$$\sigma_{kl,k} - \rho\ddot{u}_l = 0\,,\ m_{rk,r} + \varepsilon_{klr}\sigma_{lr} - \rho j\ddot{\varphi}_k = 0\,. \tag{2}$$

In (2), σ_{kl} is the stress tensor, m_{kl} is the couple stress tensor, u is the displacement vector, φ_k is the microrotation vector which in Cosserat elasticity is cinematically distinct from the macrorotation vector $r_k = 1/2\varepsilon_{klm}u_{m,l}$, and ε_{klm} is the permutation symbol. The quantity φ_k refers to the rotation of points themselves, while r_k refers to the rotation associated with movement of nearby points. In (2) ρ is the mass density and j the microinertia. The constitutive equations are

$$\sigma_{kl} = \lambda e_{rr}\delta_{kl} + (2\mu + \kappa)e_{kl} + \kappa\varepsilon_{klm}(r_m - \varphi_m) + C_1\varphi_{r,r}\delta_{kl} + C_2\varphi_{k,l} + C_3\varphi_{l,k}, \tag{3}$$

$$m_{kl} = \alpha\varphi_{r,r}\delta_{kl} + \beta\varphi_{k,l} + \gamma\varphi_{l,k} + C_1 e_{rr}\delta_{kl} + (C_2 + C_3)e_{kl} + (C_3 - C_2)\varepsilon_{klm}(r_m - \varphi_m), \tag{4}$$

where $e_{kl} = 1/2(u_{k.l} + u_{l,k})$ is the macrostrain vector. λ, and μ are Lamé elastic constants, κ is the Cosserat rotation modulus, α, β, γ, the Cosserat rotation gradient moduli, and C_i, $i = 1,2,3$ are the chiral elastic constants associated with noncentrosymmetry. For $C_i = 0$ the equations of isotropic micropolar elasticity are recovered.
For $\alpha = \beta = \gamma = \kappa = 0$, (1) reduces to the constitutive equations of classical isotropic linear elasticity theory {16]-[18].
The initial conditions are

$$u_i(x,0) = u_i^0(x), \ \varphi_i(x,0) = 0, \tag{5}$$

$$m_{ij}(x,0) = 0, \ \ \sigma_{ij}(x,0) = 0. \tag{6}$$

The touchstone of obtaining auxetic materials is that the governing equations (2) of the non-auxetic foams are invariant under geometric transformations. The equations (2) are reducing to the Helmholtz equations

$$\nabla \cdot S : \nabla U + \omega^2 U = 0, \tag{7}$$

where S is the fourth-order material tensor, ω is the wave angular frequency, $U(x,t) = U(x)\exp(-i\omega t)$, $U = (u_i, \phi_i)$, $i = 1,2,3$, $U(x,t) = U(x)\exp(-i\omega t)$.
The sonic composite layer finally consists from an array of spherical shells scatterers embedded in an epoxy matrix. The spherical shells occupy the region $R_1 < r < R_2$, $r = \sqrt{x^2 + y^2 + z^2}$, which is filled with auxetic material, and the matrix is made from an epoxy resin (Figure 3). In Figure 3, ω is the frequency of the incident sound.

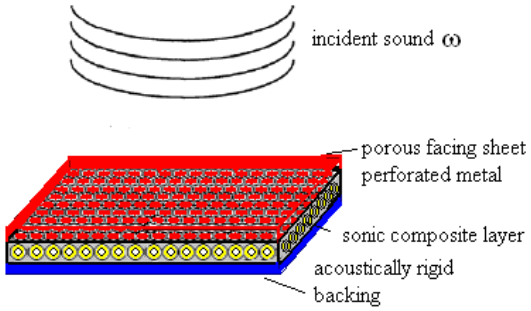

Figure 3: The sonic composite with spherical shells resonators [8].

3. EVALUATION OF THE YOUNG'S MODULUS

The overlapping of all pseudo gaps obtained from reflections on the scatterers as well as due to wave propagation in the scatterers, generates the full band-gap. Any wave is reflected completely in the frequency range where all the pseudo band-gaps for the different directions overlap. This is the fundamental mechanism for the formation of a full band-gap. Figure 4 shows the first, the second and the 210th pseudo gaps (red, blue and green zones) delimited by the attenuation peaks lines calculated along four symmetric directions, and the full band-gap (grey zone), with respect to the compressive strain. For a given compressive strain $1 - \vartheta$, this plot predicts the full band-gap.

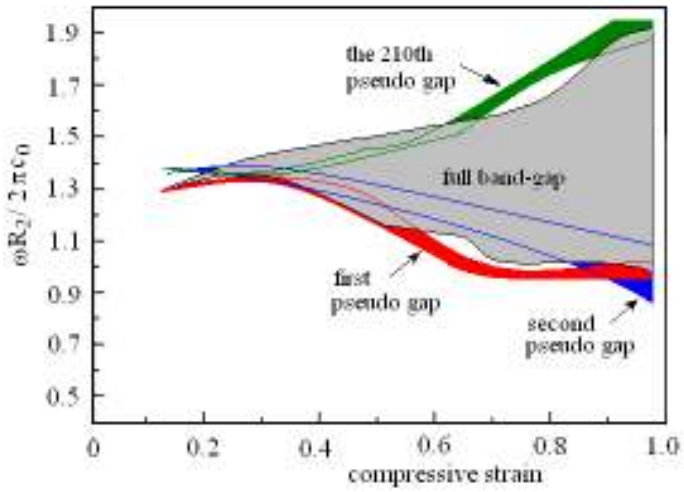

Figure 4: The full-band gap structure [8]

We are interested in the following in the knowing the influence of the Cosserat rotation modulus κ', the Cosserat rotation gradient moduli α', β', γ', and the chiral elastic constants C_i', $i = 1,2,3$, on the effective Young' modulus value of the sonic composite. The material new constants $\tilde{C} = \{\lambda', \mu', \kappa', \alpha', \beta', \gamma', C_1', C_2', C_3', \lambda_{ep}', \mu_{ep}', \kappa_{ep}'\}$ of the sonic composite consisted from an array of spherical shells scatterers embedded in an epoxy matrix, are done by the geometric transformations $dx = J_{xx'}dx'$, $J_{xx'} = \dfrac{\partial(x)}{\partial(x')}$ [8], as

$$\lambda' = \frac{\lambda}{\det(J_{xx'})},\ \mu' = \frac{\mu}{\det(J_{xx'})},\ \kappa' = \frac{\kappa}{\det(J_{xx'})},\ \alpha' = \frac{\alpha}{\det(J_{xx'})},\ \beta' = \frac{\beta}{\det(J_{xx'})},$$
$$\gamma' = \frac{\gamma}{\det(J_{xx'})},\ \rho' = \frac{\rho}{\det(J_{xx'})},\ \kappa' = \frac{\kappa}{\det(J_{xx'})},\ \rho' = \frac{\rho}{\det(J_{xx'})},\ C_i' = \frac{C_i}{\det(J_{xx'})},\ i = 1,2,3. \tag{8}$$
$$\lambda_{ep}' = \frac{\lambda_{ep}}{\det(J_{xx'})},\quad \mu_{ep}' = \frac{\mu_{ep}}{\det(J_{xx'})},\ \kappa_{ep}' = \frac{\kappa_{ep}}{\det(J_{xx'})}$$

where the index *ep* is denoting the epoxy constants. The constants have a periodical character

$$\tilde{C}(r + a) = \tilde{C}(r) \tag{9}$$

where a is the diameter of the spherical resonator. A new length scale $\eta = \dfrac{r}{\varepsilon}$ is added, where $\varepsilon > 0$ is a parameter, $\dfrac{\partial}{\partial x} = \dfrac{\partial}{\partial x} + \dfrac{1}{\varepsilon}\dfrac{\partial}{\partial \eta}$. The problem of Bécus homogenization via multiple scale expansion consists in studying (7) as $\varepsilon \to 0$ [6, 19]. As $\varepsilon \to 0$, the periodic variations of $\tilde{C}$ become frequent, so that the study of equations will bring information on the solutions for different values a. We find

$$E = F(\tilde{C}) + \frac{1}{3}\gamma + \frac{1}{2}\tilde{p}^2 + \frac{3}{4}\sqrt{\delta}\tilde{p}, \tag{9}$$

where

$$\gamma = \frac{(2\mu' + \kappa')(3\lambda' + 2\mu' + \kappa_{aux})}{(2\lambda' + 2\mu' + \kappa_{aux})},\quad \delta = \frac{(2\mu' + \kappa')(3\alpha' + 2\beta' + \gamma')}{(2C_1' + 2C_2' + C_3')},\quad \tilde{p}^2 = \frac{2\kappa_{aux}}{\zeta},$$

$$\zeta = \frac{(C_{1aux} + 3C_{2aux} + C_{3aux})(3\lambda' + 2\mu' + \kappa_{aux})}{(\lambda_{aux} + 2\mu_{aux} + \kappa_{aux})(\alpha_{aux} + 2\beta_{aux} + \gamma_{aux})}. \tag{10}$$

The function $F(\tilde{C})$ is numerically determined only. The most important physical parameter which dominates the negative Poisson's ratio transformation is the compression ratio $\vartheta = \frac{(R_2'^3 - R_1'^3)}{R_2^3}$, where prime denotes the final parameters. This parameter is directly related to the capacity of damping of the sonic composite. The qiuantity $1-\vartheta$ represents the compressive strain.

Figure 5 represents the variation of the homogenized Young's modulus with respect to the compressive strain $1-\vartheta$, and the Poisson's ratio ν of the auxetic material. In the simulation, the spherical specimen has $R_2 = 15$mm the initial radius, and $\lambda = 2.59$GPa, $\mu = 0.77$GPa, $\kappa = 0.0144$GPa, $\alpha = 1.77 \times 10^4$ N, $\beta = 3.37 \times 10^4$ N, $\gamma = 0.33 \times 10^4$ N, $C_1 = -0.5 \times 10^4$ N/m, $C_2 = -2.9 \times 10^4$ N/m, $C_3 = -6.8 \times 10^4$ N/m.

The radius R_1 depends on ϑ. So, for $\vartheta = 0.25$, $R_1 = 13.63$ mm, for $\vartheta = 0.3$, $R_1 = 13.32$ mm, for $\vartheta = 0.35$, $R_1 = 12.99$ mm, and for $\vartheta = 0.4$, $R_1 = 12.65$ mm, respectively.

We observe that Young's modulus is increasing and decreasing in a complex way. The Poisson's ratio significanntly depends on the compressive strain.

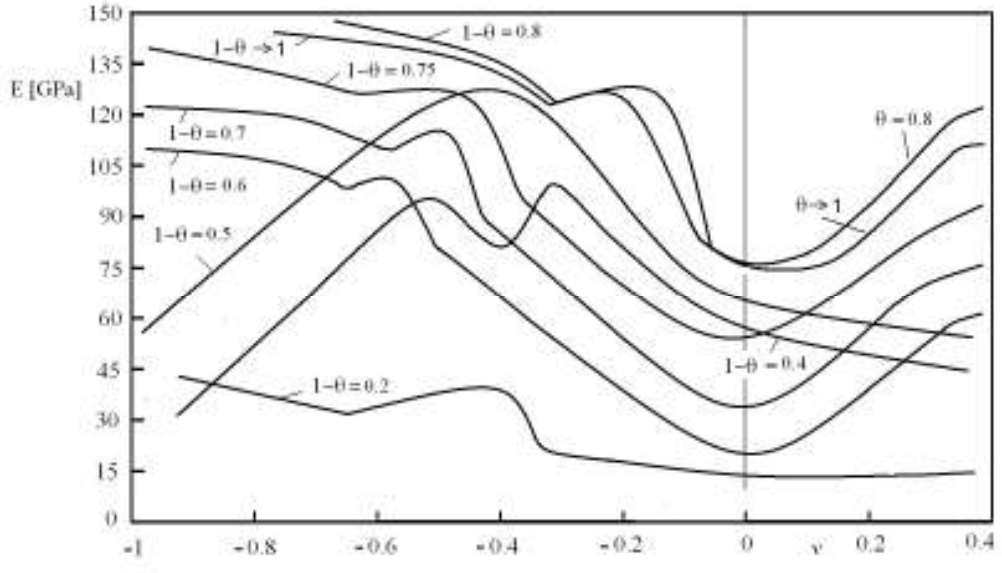

Figure5: The homogenized Young's modulus variation with respect to Poisson's ratio of the auxetic material and the compressive strain

ACKNOWLEDGEMENT.

The authors gratefully acknowledge the financial support of the National Authority for Scientific Research ANCS/UEFISCDI through the project PN-II-ID-PCE-2012-4-0023.

REFERENCES

[1] Donescu, Şt., Chiroiu, V., Munteanu, L., *On the Young's modulus of a auxetic composite structure*, Mechanics Research Communications, 36, 294-301, 2009.

[2] Munteanu, L., Chiroiu, V., Dumitriu, D., Beldiman, M., *On the characterization of auxetic composites*, Proceedings of the Romanian Academy, Series A: Mathematics, Physics, Technical Sciences, Information Science, 9(1), 33-40, 2008.

[3] Lakes, R.S., *Experimental micro mechanics methods for conventional and negative Poisson's ratio cellular solids as Cosserat continua*, J. Engineering Materials and Technology, 113, 148–155, 1991.

[4] Lakes, R.S., *Foam structures with a negative Poisson's ratio*, Science, 235, 1038–1040, 1987.

[5] Lakes, R.S., *Experimental microelasticity of two porous solids*, Int. J. Solids, Structures, 22, 1986, pp.55–63, 1986.

[6] Munteanu, L., Dumitriu, D., Donescu, Şt., Chiroiu, V., *On the complexity of the auxetic systems*, Proc.of the European Computing Conference, Lecture Notes in Electrical Engineering 2(28), 1543-1549, Springer-Verlag (eds. N.Mastorakis, V.Mladenov), 2009.
[7] Munteanu, L., Chiroiu, V., *On the dynamics of locally resonant sonic composites*, European Journal of Mechanics-A/Solids, 29(5), 871–878, 2010.
[8] Munteanu L., Chiroiu V., *On the response of a sonic liner under severe acoustic loads*, European Journal of Mechanics-A/Solids, 2013 (in press).
[9] Hirsekorn, M., Delsanto, P.P., Batra, N.K., Matic, P., *Modelling and simulation of acoustic wave propagation in locally resonant sonic materials*, Ultrasonics, 42, 231–235, 2004.
[10] Munteanu L., *Nanocomposites*, Editura Academiei, 2012.
[11] Cosserat, E., and F., *Theorie des Corps Deformables*, Hermann et Fils, Paris, 1909.
[12] Eringen, A.C., *Linear Theory of Micropolar Elasticity*, J. Math. & Mech., 15, 909–924, 1966.
[13] Eringen, A.C., *Theory of micropolar elasticity*, in Fracture (ed. R.Liebowitz), Academic Press, 2, .621–729, 1968.
[14] Mindlin, R.D., *Microstructure in linear elasticity*, Arch. Rat. Mech. Anal., 16, 51–78, 1964.
[15] Mindlin, R.D., *Stress functions for a Cosserat continuum*, Int J. Solids Structures, **1**, 265–271, 1965.
[16] Gauthier, R.D., *Experimental investigations on micropolar media*, 395–463, in: Mechanics of Micropolar Media, World scientific, 1982.
[17] Teodorescu, P.P., Munteanu, L., Chiroiu, V., *On the wave propagation in chiral media*, New Trends in Continuum Mechanics, Ed. Thetha Foundation, Bucharest, 303–310, 2005.
[18] Teodorescu, P.P., Badea, T., Munteanu, L., Onişoru, J., *On the wave propagation in composite materials with a negative stiffness phase*, New Trends in Continuum Mechanics, Ed. Thetha Foundation, Bucharest, 295–302, 2005.
[19] Bécus, G.A., *Homogenization and random evolutions: Applications to the mechanics of composite materials*, Quarterly of Applied Mathematics, XXXVII (3), 209–217, 1979.